

# NATIONAL AIR INTELLIGENCE CENTER



THE EFFECTS OF TRANSVERSE MOTION ON  
ELECTRON BACK BOMBARDMENT IN  
STANDING WAVE LINEAR ACCELERATORS

by

Gu Benguang, Wang Huizhang



Approved for public release:  
distribution unlimited

19960104 045

**HUMAN TRANSLATION**

NAIC-ID(RS)T-0367-95 8 November 1995

MICROFICHE NR: 95C000699

THE EFFECTS OF TRANSVERSE MOTION ON  
ELECTRON BACK BOMBARDMENT IN  
STANDING WAVE LINEAR ACCELERATORS

By: Gu Benguang, Wang Huizhang

English pages: 13

Source: Qiangjiguang Yu Zizishu, Vol. 5, Nr. 4,  
November 1993

Country of origin: China  
Translated by: Edward A. Suter  
Requester: NAIC/TATD/Dr. James Newton  
Approved for public release: distribution unlimited.

Accession For	
NTIS CRA&I	<input checked="" type="checkbox"/>
DTIC TAB	<input type="checkbox"/>
Unannounced	<input type="checkbox"/>
Justification	
By _____	
Distribution /	
Availability Codes	
Dist	Avail and/or Special
A-1	

<p>THIS TRANSLATION IS A RENDITION OF THE ORIGINAL FOREIGN TEXT WITHOUT ANY ANALYTICAL OR EDITORIAL COMMENT STATEMENTS OR THEORIES ADVOCATED OR IMPLIED ARE THOSE OF THE SOURCE AND DO NOT NECESSARILY REFLECT THE POSITION OR OPINION OF THE NATIONAL AIR INTELLIGENCE CENTER.</p>	<p>PREPARED BY: TRANSLATION SERVICES NATIONAL AIR INTELLIGENCE CENTER WPAFB, OHIO</p>
---	---

*High Power Laser and Particle Beams (Qiangguang Yu Lizishu)*

Vol. 5, No. 4 Nov., 1993

## THE EFFECTS OF TRANSVERSE MOTION ON ELECTRON BACK BOMBARDMENT IN STANDING WAVE LINEAR ACCELERATORS

(Romanized title: "*Hengxiang Yundong Dui Zhubo Jiasuguan  
Dianzi Fanhong De Yingxiang*")

by Gu Benguang and Wang Huizhang  
(Beijing Medical Equipment Institute, Beijing, 100011)

**Abstract:** Electron back-bombardment in standing wave linear accelerators [linacs] is an undesirable phenomenon which can cause the electron gun cathode to overheat and destroy electron optics. It is related not only to longitudinal motion factors, but also to transverse motion factors. In this paper, the authors analyze the effects of transverse motion on electron back-bombardment and point out that owing to transverse motion, only part of the backward-motion electrons can back-bombard the electron gun cathode surface. The authors provide methods for calculating back-bombardment beam envelopes, back-bombardment ratios, back-bombardment currents, and back-bombardment power.

**Key terms:** electron back-bombardment, transverse motion, standing wave accelerating tube

### 1. Introduction

The standing wave accelerating tubes in modern standing wave linear accelerators use two- or three-period resonant couplings in their standing wave accelerating structures. They are made up of a series of accelerating cavities and coupling cavities which are coupled to each other. The accelerating cavity located at the beginning of accelerating tubes

is called the leading cavity. Changes in motion of injected electrons primarily take place at the stage where velocity is low, i.e., in the leading cavity. It is possible for changes in direction of motion to take place in successive accelerating cavities, but there are few opportunities for [electrons] to return to their initial positions in the leading cavity and strike against the cathode surface. Therefore, this paper only discusses and analyzes what happens in the leading cavity.

No matter whether electrons are moving forward or backward, because some electrons with excessively large radial displacement will be lost when they strike against the cavity wall or the beam hole wall, when considering the effects of transverse motion, it is necessary to carry out a three-dimensional analysis and to separate overall average emission current  $i_E$  into three categories: accelerating current  $i_A$ , which ultimately moves forward and can enter the next accelerating cavity through the ejection beam hole; current lost against walls  $i_w$ , which is current in either forward or backward motion that is lost against cavity walls or beam hole walls; and back-bombardment current  $i_c$ , which is current that moves backward and can back-bombard the cathode surface. Here,  $i_E = i_A + i_w + i_c$ .

Clearly, accelerating current  $i_A$  is only part of forward current ( $i_F$ ), and back-bombardment current  $i_c$  is only part of backward current ( $i_B$ ). Moreover, under three-dimensional motion conditions, it is necessary to redefine parameters relevant to capture and back-bombardment. To this end, capture rate  $k_A$  is defined as the ratio of accelerating current  $i_A$  to overall emission current  $i_E$ ; back-bombardment rate [ $k_c$ ] is defined as the ratio of back-bombardment current  $i_c$  to overall emission current  $i_E$ ; and back-bombardment power  $P_c$  is defined as the power of electrons that back-bombard the cathode surface.

$$k_A = \frac{i_A}{i_E} \quad (1)$$

$$k_c = \frac{i_c}{i_E} \quad (2)$$

To calculate  $i_c$ ,  $k_c$ , and  $P_c$ , it is necessary to calculate transverse motion of backward motion.

There exist many methods for calculating transverse motion of forward motion. Among them, equations and methods to derive beam envelope are better for understanding the overall variations in a beam. Therefore, when calculating transverse motion of back-

bombardment motion, the authors of this paper also use these methods.

Page 609

We assume that a corresponding injection phase  $\varphi_0$  electron ultimately makes a backward motion, its beam envelope radius upon returning to its initial position is  $R_B(\varphi_0)$ , and its injection beam hole radius is  $R_c$ . (Since the cathode radius is often greater than  $R_c$ , as long as a backward-moving electron passes through the beam hole, it can back-bombard the cathode surface). We also assume that electric charges are evenly distributed within the beam envelope. Then, when  $R_B(\varphi_0) \leq R_c$ , all of the backward motion electrons can back-bombard the cathode surface, and when  $R_B(\varphi_0) > R_c$ , only part of the backward motion electrons can back-bombard the cathode surface. Thus, we can extract:

$$i_c = \frac{i_E}{2\pi} \int_{\Delta\varphi_0} F\left(\frac{R_c}{R_B(\varphi_0)}\right) d\varphi_0 \quad (3)$$

$$k_c = \frac{1}{2\pi} \int_{\Delta\varphi_0} F\left(\frac{R_c}{R_B(\varphi_0)}\right) d\varphi_0 \quad (4)$$

$$P_c = \frac{i_E}{2\pi e} \int_{\Delta\varphi_0} F\left(\frac{R_c}{R_B(\varphi_0)}\right) W(\varphi_0) d\varphi_0 \quad (5)$$

where function  $F(x)$  in the integral is defined as:

$$F(x) = \begin{cases} 1 & \text{当 } x \geq 1 \\ x^2 & \text{当 } x < 1 \end{cases}$$

**Key:** (1). when

By solving the beam envelope equation of backward motion, after obtaining  $R_B(\varphi_0)$ , it is possible to calculate  $i_c$ ,  $k_c$ , and  $P_c$ .

## 2. Beam envelope equations for backward motion

Beam envelope equations were first applied to proton linacs in 1959. They were

called the K-V equations<sup>[2]</sup>. In 1978, application of these equations was extended to traveling wave electron linacs<sup>[3]</sup>. Still later, their use spread to standing wave electron linacs<sup>[4]</sup>.

The equations for radial direction motion and beam envelope of standing wave electron linacs are, respectively,

$$\frac{dP_r}{dz} + N(z)r = 0 \quad (6)$$

$$\frac{d^2 R}{dz^2} + \frac{1}{\beta^2 \gamma} \frac{d\gamma}{dz} \frac{dR}{dz} + \frac{N(z)}{\beta \gamma} R - \frac{\epsilon_n}{(\beta \gamma)^2 R^3} = 0 \quad (7)$$

where

$$N(z) = \frac{e E_r(z)}{\beta m_0 c^2} \sin(\varphi + \varphi_0) + \frac{e \mu_0 H_\theta(z)}{m_0 c} \cos(\varphi + \varphi_0) + \frac{1}{4\beta\gamma} \left( \frac{e \mu_0 H_z(z)}{m_0 c} \right)^2 - \frac{3e I t_s \mu_r}{4\pi \epsilon_0 m_0 c^2 \beta \gamma^2 r_s^2 a_s} \quad (8)$$

$$\beta = \frac{v}{c} \approx \frac{dz}{cdt}, \quad \gamma = \frac{m}{m_0}$$

In these formulas,  $z$ ,  $r$ ,  $\theta$ , and  $v$  are, respectively, electrons' axial direction, radial<sup>1</sup> direction, radial coordinates, and velocity;  $e$ ,  $m_0$ , and  $m$  are the electrons' electric charge, rest mass, and mass;  $c$ ,  $\epsilon_0$ , and  $\mu_0$  are the speed of light in a vacuum, vacuum dielectric constant, and vacuum magnetic inductivity;  $I$ ,  $\mu_r$ ,  $a_s$ ,  $r_s$ , and  $t_s$  are beam intensity, beam cluster<sup>2</sup> ellipsoidal factor, beam cluster equivalent ellipsoidal major axis, minor axis, and flight time between two adjacent beam clusters;  $E_r(z)$  and  $H_\theta(z)$  are radio frequency radial direction electric field component and radial magnetic field component at a value of  $r=1\text{mm}$ ;  $H_z(z)$  is the externally appended radial direct current magnetic field;  $\varphi_0$  and  $\varphi$  are injection phase and phase increment of electrons in the radio frequency field; and  $\epsilon_n$  and  $R$  are normalized transverse emittance and beam envelope radius.

<sup>1</sup> Note that there are two Chinese words used for "radial," *fuxiang* ( $\theta$ ) and *jingxiang* ( $r$ ). To distinguish between the two, I have translated  $\theta$  as "radial" and  $r$  as "radial direction."

<sup>2</sup> No translation was found for *shutuan*, which I call "beam cluster" here. It could mean "beam group" or simply "beam."

Formerly, solving for beam envelope equations was limited only to forward motion; that is, consideration was only given to situations where  $dz > 0$  and  $\beta > 0$ . But when solving for envelope equations of backward motion, consideration should be given to situations where  $dz < 0$  and  $\beta < 0$ .

In radial direction motion equation (6), the difference between backward motion and forward motion is primarily manifested as changes in coefficient  $N(z)$ . When  $dz < 0$  and  $\beta < 0$ , a change takes place in the sign [i.e., positive or negative] of item  $H_0$  contained in  $N(z)$ , while other items' signs do not change as direction changes. This happens because the radial direction forces produced by items  $E_r$ ,  $H_z$  and  $I$  are all unrelated to direction of motion; only the radial direction force produced by item  $H_0$  is related to direction of motion. But when the  $\beta$  value of electrons in the leading cavity is small and the radial direction applied force produced by item  $H_0$  is small, the overall direction of radial direction applied force is basically determined by item  $E_r$ .

In beam envelope equation (7), in addition to paying attention to changes in direction of motion that lead to variations in  $N(z)$ , [we] should also pay attention to the coefficient of item  $dR/dz$ , which changes along with  $d\gamma/dz$ . During forward and backward accelerating motion,  $d\gamma/dz > 0$ , and during forward and backward decelerating motion,  $d\gamma/dz < 0$ .

The above analyses show that when backward motion occurs, although signs of certain coefficients may change, it is still possible to use methods for solving for forward motion to solve radial direction motion of backward motion equations and beam envelope equations.

A special situation takes place at the instant when the direction of motion changes. In the instant when  $\beta > 0$  changes to  $\beta < 0$  or  $\beta < 0$  changes to  $\beta > 0$ , situations where  $dz = 0$  and  $\beta = 0$  occur. At this time, there are several equation coefficients that tend to be infinitely large, and this causes difficulties in mathematical solution to take place. But from the perspective of physics, because it is impossible for the beam envelope radius to diverge in an instant, when we carry out concrete step-by-step calculations and encounter special situations where  $dz = 0$  and  $\beta = 0$ , we must think of ways to replace 0 with an appropriately small amount. The sign chosen is determined according to the tendency of motion. If

motion was originally forward, the sign chosen [for the amount] is negative; otherwise, the sign chosen is positive. By using this processing method, we have concretely calculated the beam envelope changes of several standing wave accelerating tubes under different injection phase conditions. Calculated results have corresponded to the analysis of the physics process, as expected.

### 3. Transverse motion factors that affect electron back-bombardment

The accelerating cavities of most standing wave accelerating tubes are Los Alamos-type accelerating cavities with a working mode of  $TM_{010}$ . In order to understand the effects of transverse motion factors on electron back-bombardment, these effects are analyzed and discussed below through specific calculations of a 6MeV short standing wave accelerating tube<sup>[5]</sup>.

#### 3.1 Effects of radio frequency electromagnetic fields

Figure 1 is a distribution graph showing axial electric field component amplitude  $E_z(z)$  ( $r=0$ ), radial direction electric field component amplitude  $E_r(z)$  ( $r=1\text{mm}$ ), and radial magnetic field component amplitude  $H_\theta(z)$  ( $r=1\text{mm}$ ) along the axis in the leading cavity of the above-mentioned standing wave accelerating tube. The first five millimeters of this leading cavity is the injection beam hole, and the following 11 millimeters is the ejection beam hole. From the distribution curve, one can tell that the leading cavity is an asymmetrical cavity.

Figure 2 shows the phase variation of different injected phase electrons in this leading cavity. The abscissa is axial coordinate  $z$ , the part above the abscissa represents the positive phase region ( $0^\circ - 180^\circ$ ), and the part below represents the negative phase region ( $-180^\circ - 0^\circ$ ). One can tell that after most of the electrons in the negative injection phase region are subjected to a brief decelerating effect, they quickly move to the positive phase region ( $0^\circ - 90^\circ$ ) to gain acceleration, while after most electrons in the positive injection phase region are subjected to a brief accelerating effect, they quickly move to the negative phase region to be subjected to decelerating and backward accelerating effects. The phases of these electrons that are finally in backward motion ultimately converge in the  $-90^\circ - 90^\circ$  range.

Figure 3 shows the energy gained by injection phase electrons in the leading cavity of the standing wave accelerating tube. The abscissa is injection phase  $\varphi_0$ , the coordinates above the abscissa represent forward energy, and the coordinates below the abscissa represent backward energy. One can tell that the injection phase range  $\Delta\varphi_F$  [of electrons] that capture forward energy is located in the negative injection phase region, while the injection phase range  $\Delta\varphi_B$  [of electrons] that capture backward energy is located in the positive injection phase region. The same holds true for most standing wave accelerating tubes.

Figure 4 shows the axial electric field component applied force received by different injection phase electrons which are in the process of motion in the leading cavity, [expressed as]  $eE_z(z)\sin(\varphi + \varphi_0)$ . The abscissa is  $z$ . Above the abscissa,  $eE_z(z)\sin(\varphi + \varphi_0) > 0$ , which is equivalent to the accelerating effect, and below the abscissa,  $eE_z(z)\sin(\varphi + \varphi_0) < 0$ , which is equivalent to decelerating or backward accelerating effects. In the figure,  $+60^\circ$  and  $+120^\circ$  are taken as representative in the positive injection phase region, and  $-60^\circ$  and  $-120^\circ$  are taken as representative in the negative injection phase region.

Page 611

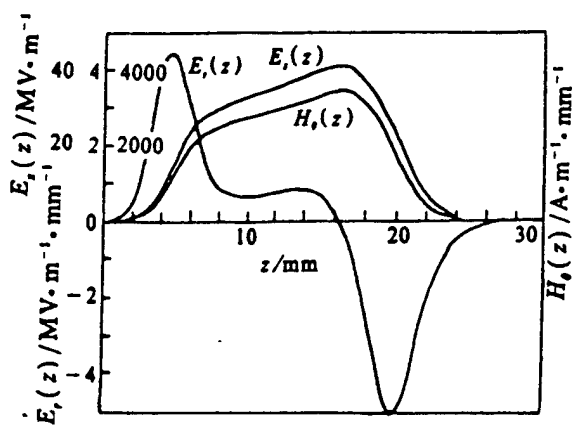


Fig. 1 Distribution of field amplitude  $E(z)$ ,  $E_z(z)$ ,  $H_z(z)$

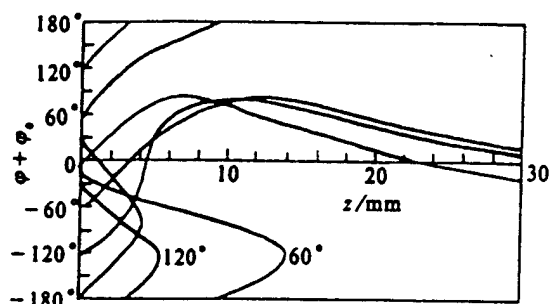


Fig. 2 Phase variation

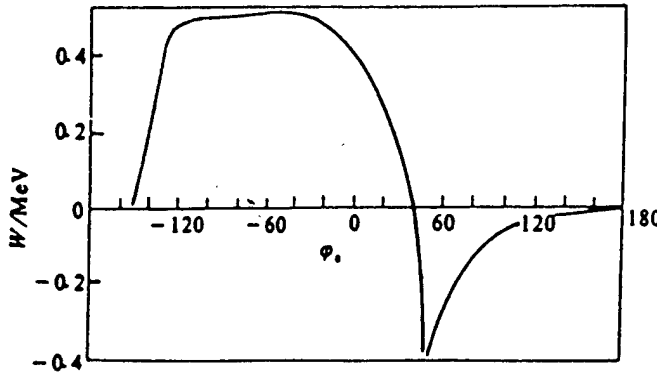


Fig. 3 Output energy vs injection phase

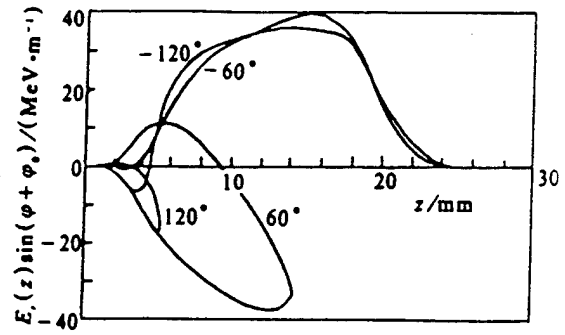


Fig. 4 Variation of axial force produced by  $E_r(z)$

Figure 5 shows the radial direction force produced by radial direction electric field component which is received by different injection phase electrons that are in the process of motion in the leading cavity. [It is expressed as]  $-eE_r(z)r\sin(\varphi + \varphi_0)$ . The abscissa is  $z$ , and above the abscissa  $-eE_r(z)r\sin(\varphi + \varphi_0) > 0$ , which is equivalent to a defocusing effect. Below the abscissa,  $-eE_r(z)r\sin(\varphi + \varphi_0) < 0$ , which is equivalent to a focusing effect. Clearly, the direction of radial direction force produced by the radial direction electric field component is related to radio frequency phase and the direction of  $E_r$ . It is clear from Figure 5 that electrons that gain forward energy in the first half of the leading cavity begin to be affected by decelerating effects in the negative phase region; here,  $-eE_r(z)r\sin(\varphi + \varphi_0) > 0$ . Following this, when the electrons enter the positive phase region,  $-eE_r(z)r\sin(\varphi + \varphi_0) < 0$ . When the electrons enter the latter half of the leading cavity, although they are located in a positive phase region,  $-eE_r(z)r\sin(\varphi + \varphi_0) > 0$  because the direction of  $E_r$  changes. The entire process is as follows: defocusing – focusing – defocusing. Most electron motion of gaining backward energy takes place in the front half of the leading cavity. [Electrons] begin to be subjected to accelerating effects in the positive phase region, where  $-eE_r(z)r\sin(\varphi + \varphi_0) < 0$ . Afterwards, as they continue their forward motion, [electrons] are subjected to decelerating effects, whereupon  $-eE_r(z)r\sin(\varphi + \varphi_0) > 0$ . After electron motion turns backward, [electrons] in the negative phase region are subjected to backward accelerating effects, and  $-eE_r(z)r\sin(\varphi + \varphi_0) < 0$ . The whole process is as follows: focusing – defocusing – defocusing.

Figure 6 shows the radial direction force produced by radial magnetic field component that different injection phase electrons in the process of motion in this leading

cavity receive, [expressed as]  $-e\mu_0 c \beta H_0(z) r \cos(\varphi + \varphi_0)$ . The abscissa is  $z$ . Above the abscissa,  $-e\mu_0 c \beta H_0(z) r \cos(\varphi + \varphi_0) > 0$ , which is equivalent to the defocusing effect, and below the abscissa,  $-e\mu_0 c \beta H_0(z) r \cos(\varphi + \varphi_0) < 0$ , which is equivalent to the focusing effect.

Page 612

Obviously, in addition to being related to radio frequency phase and  $H_0$  amplitude, the radial direction force produced by radio frequency magnetic field component is also related to  $\beta$ . One can see from Figure 6 that for electrons that gain forward energy, besides those electrons with injection phases between  $-180^\circ$  and  $-90^\circ$  which begin to have a section where  $-e\mu_0 c \beta H_0(z) r \cos(\varphi + \varphi_0) > 0$ , electrons with injection phases ranging between  $-90^\circ$  and  $90^\circ$  always have  $-e\mu_0 c \beta H_0(z) r \cos(\varphi + \varphi_0) < 0$ . The entire process is one of either focusing–defocusing or defocusing–defocusing. Among electrons that capture backward energy, besides those electrons with injection phases in the range between  $0^\circ$  and  $90^\circ$  which begin to have a section where  $-e\mu_0 c \beta H_0(z) r \cos(\varphi + \varphi_0) < 0$ , other electrons with injection phases ranging between  $90^\circ$  and  $180^\circ$  or between  $-90^\circ$  and  $-180^\circ$  all begin to have  $-e\mu_0 c \beta H_0(z) r \cos(\varphi + \varphi_0) > 0$ . After direction of electron motion changes, this becomes  $-e\mu_0 c \beta H_0(z) r \cos(\varphi + \varphi_0) < 0$ , and further, when electron phase moves to the range between  $-90^\circ$  and  $90^\circ$ , it changes again to  $-e\mu_0 c \beta H_0(z) r \cos(\varphi + \varphi_0) > 0$ . The entire process is one of either focusing–defocusing–focusing–defocusing, or defocusing–focusing–defocusing.

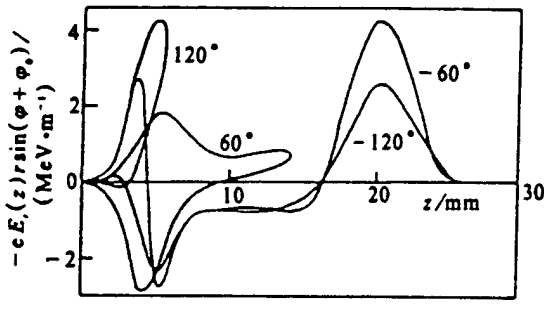


Fig. 5 Variation of radial force produced by  $E_r(z)$

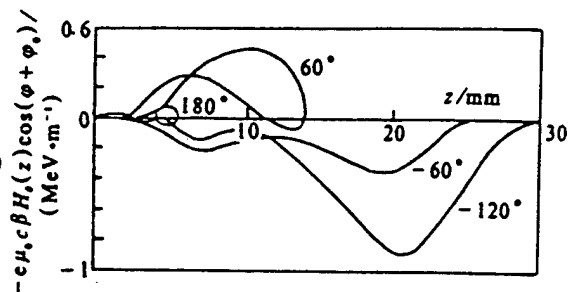


Fig. 6 Variation of radial force produced by  $H_r(z)$

Figure 7 depicts the combined radial direction force produced by radio frequency radial direction electric field component and radio frequency radial magnetic field

component, expressed as  $-er[E_r(z)\sin(\varphi + \varphi_0) + \mu_0 c \beta H_0(z)\cos(\varphi + \varphi_0)]$ . One can tell that its variations are basically similar to those of Figure 5. Figure 7 lets us see that aside from where the radio frequency electromagnetic field causes electrons that capture backward energy to begin to have a section of focusing effects, most of the rest of the process has a defocusing effect. Defocusing effects during the process of backward motion have an especially significant influence on electron back-bombardment. Clearly, the greater the radio frequency radial direction electric field component at the entrance to the leading cavity is, the stronger this defocusing effect is.

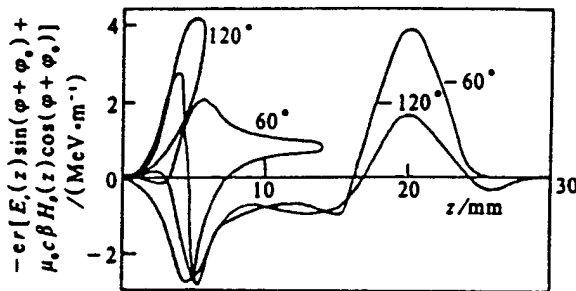


Fig. 7 Variation of radial force produced by  $E_r(z)$  and  $H_0(z)$

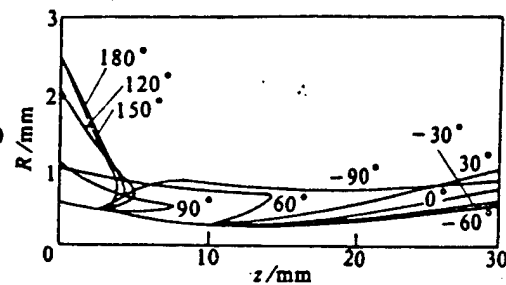


Fig. 8 Variation of beam envelope under forward and backward motions

### 3.2 The effects of externally attached direct current magnetic fields

By attaching solenoid coils to the outside of the standing wave accelerating tube, it is possible to produce additional axial direct current electromagnetic fields inside the accelerating cavity. Usually, because the accelerating gradient of short standing wave accelerating tubes is high, electrons quickly attain relativistic velocity, and it is generally unnecessary to attach solenoid coils.

Page 613

[However,] it is sometimes necessary to attach solenoid coils to the beginning part of longer standing wave accelerating tubes.

No matter if the electrons in the accelerating cavity are in forward or backward

motion, axial direct current magnetic fields have a focusing effect on electrons. This is because the axial direct current magnetic field only produces additional Lorentz forces on electrons with a tendency to deviate from the axis center, no matter what the direction of motion of the electrons is.

Thus, the use of externally attached axial direct current magnetic fields can not only cause the capture rate to rise, it can also cause the back-bombardment rate to rise.

The method of attaching transverse coils to the outside of microwave electron guns proposed by C.B. McKee and J.M. Madey can also be applied to standing wave accelerating tubes. After attaching a transverse direct current magnetic field to the inside of the accelerating cavity, it is possible to cause electrons that capture backward energy to deviate from the beam's central axis during the process of backward motion, causing the electrons to be unable to directly back-bombard the cathode surface. However, the drawback to this is that adding a transverse direct current magnetic field will at the same time cause electrons that capture forward energy to deviate from the beam's central axis during the process of forward motion. To correct the motion trajectories of electrons that capture forward energy in succeeding accelerating cavities, it is necessary to install several correcting coils at appropriate places in succeeding cavities.

### **3.3 The effects of beam cluster space charges**

When electron velocity is low, the charges of beam cluster internal space primarily have a static electric field repulsion effect. Their overall effect is one of defocusing. As electron velocity increases, the defocusing effect gradually weakens.

There is a process of change from positive to negative of the electronic velocity of electrons that capture backward energy. Their space charges are also continuously varying, and in general, variation is greatest when direction of motion changes.

Increasing the intensity of the beam will cause the beam envelope radius to increase at the same time during the processes of forward and backward motion, and may cause back-bombardment rate to fall and back-bombardment power to rise.

Figure 8 shows the process of variation of the beam envelope in the leading cavity

at different injection phases. It is assumed here that the injection electrons have a small initial emittance and are injected at a negative injection angle. In this calculation, [we] considered the effect of the beam space charge, but assumed at the beginning that there was no externally attached direct current magnetic field. From Figure 8, one can tell that the beam envelope of the electrons that capture forward energy is convergent at the outset, but gradually diverges in the latter half of the leading cavity; [also,] the beam envelope of the electrons that capture backward energy in the process of forward motion is convergent, but in the process of backward motion, it exhibits strong divergence. When compared with Figure 7, it is easy to see that the variation process of the beam envelope and the variation process of radial direction force correspond.

#### 4. Conclusions

In light of the above analyses and calculations, the effects of transverse motion factors on electron back-bombardment in the standing wave accelerating tube can be summed up as follows:

1. Because, during transverse motion, some of the electrons in backward motion will strike the walls of either the leading cavity or the injection beam hole, reducing the radius of the injection beam hole of the standing wave accelerating tube and increasing the length of the injection beam hole when possible will help lower the back-bombardment ratio.

2. The greater the radio frequency electromagnetic field radial direction force in the leading cavity is, the greater the beam envelope radius of electrons in forward and backward motion will be, and the lower the rate of back-bombardment will be, but, at the same time, the beam divergence of forward motion will increase.

3. External attachment of axial direct current magnetic fields will cause the beam envelope radius of forward and negative motion to shrink and make the back-bombardment ratio rise.

4. An increase in space charge force will cause the beam envelope radius of forward and backward motion to increase and the back-bombardment ratio to decrease, but will have a negative effect on forward motion.

Reference Documents

- [1] Gu, B. et al. *High Power Laser and Particle Beams*, 1991, 3(3):286-296.
- [2] Kapkinskij, M., Vladimirskij, V. International Conference on High Energy Accelerators and Instrumentation, CERN, 1959, 274.
- [3] Xie, Y. et al. *Yuanzineng Kexue Jishu (Atomic Energy Science and Technology)*, 1978, 2:119-126.
- [4] Lin, Y. et al. *High Power Laser and Particle Beams*, 1990, 2(4):431-441.
- [5] Gu, B. et al. *Atomic Energy Science and Technology*, 1993, 27(1):23-28.

DISTRIBUTION LIST

DISTRIBUTION DIRECT TO RECIPIENT

<u>ORGANIZATION</u>	<u>MICROFICHE</u>
B085 DIA/RTS-2FI	1
C509 BALL0C509 BALLISTIC RES LAB	1
C510 R&T LABS/AVEADCOM	1
C513 ARRADCOM	1
C535 AVRADCOM/TSARCOM	1
C539 TRASANA	1
Q592 FSTC	4
Q619 MSIC REDSTONE	1
Q008 NTIC	1
Q043 AFMIC-IS	1
E404 AEDC/DOF	1
E410 AFDIC/IN	1
E429 SD/IND	1
P005 DOE/ISA/DDI	1
1051 AFIT/LDE	1
PO90 NSA/CDB	1

Microfiche Nbr: FID95C000699  
NAIC-ID(RS)T-0367-95